CHEMIJA. 2004. T. 15. Nr. 4. P. 22–28

Pulse and reverse plating effect on the structure and corrosion properties of Zn and Zn alloy coatings. 1. Zn–Ni

Laima Gudavièiûtë, Aleksandras Kalinièenko, Remigijus Juðkënas, Rimantas Ramanauskas

Institute of Chemistry, A. Goštauto 9, LT-01108 Vilnius, Lithuania

The influence of pulse plating parameters on the surface morphology, grain size, lattice imperfection and corrosion properties of Zn–Ni alloy was studied. The coatings were electrodeposited in alkaline cyanide-free solution containing glycerine complex Ni ions. AFM was applied for surface morphology examination, XRD measurements were carried out for phase composition and texture analysis, while electrochemical techniques were used for corrosion behaviour studies. The pulse plated Zn–Ni coatings appeared to consist of the γ-$Zn_{21}Ni_5$ phase; the composition of the latter depended on the plating parameters. The alloy lattice imperfection and grain size were established to be the main factors determining corrosion behaviour of the coating.

Key words: Zn and Zn alloys, electrodeposits, structure, corrosion

INTRODUCTION

Under increasing requirements of industry (especially automotive) to reduce coating thickness and to prolong the service life of a coated material, the corrosion resistance of sacrificial coatings on steel needs to be enhanced. Extensive attempts have been taken recently to develop highly corrosion resistant coatings on steel. As a result, the conventional zinc electroplates are being replaced by zinc alloys. It has been stated in several studies [1–8] that corrosion resistance of electrodeposited Zn–Ni alloy coatings within a certain composition range (9–15 wt.%) can be significantly higher (5–6 times) than that for pure zinc [8].

Electrodeposited Zn–Ni alloys exist in the form of three dominant phases: α, γ and η. The α-phase is a solid solution of Zn in Ni with an equilibrium solubility of about 30% Zn. The η-phase is a solid solution of Ni in Zn, with a Ni solubility of less than 1%. The composition range of the pure γ-single phase was determined to be between 10 and 30% Ni. The amount of Ni in the alloy, which finds industrial application in the corrosion protection field, is around 15% and its dominant structure is the γ- phase $Zn_{21}Ni_5$ [8].

It was revealed in our previous works, *e.g.*, [5, 9–11], that metal structure is an important parameter, which under certain conditions can be the main factor determining corrosion behaviour of Zn alloys. Modification of the Zn–Ni alloys' structure, therefore, may be the way to create new more resistant coatings on steel.

Pulse electrodeposition can be used as a means to produce a unique structure, *i.e.* coatings with properties not obtained by direct current (d.c.) plating. Pulse electrodeposition yields a finer-grained and more homogeneous surface appearance of the deposit, because a higher instantaneous current density is possible during deposition by using pulse control in comparison with that by d.c. plating.

Acidic or alkaline plating baths can be used for Zn–Ni alloy deposition. Data on pulse plated Zn–Ni alloy published up to date deal with the coatings deposited from acidic solutions [8, 12, 13]. Electrodeposition of this alloy in acidic bath, especially under d.c. conditions, results in the dual phase structure formation [14], which implies an unsatisfactory corrosion resistance of the coating. Meanwhile, deposition in alkaline solutions, in contrast to acidic ones, is less efficient but gives a more uniform plating and results in the γ-single phase formation [9, 11].

The objective of the present investigation was to determine the influence of pulse electrodeposition parameters on the surface morphology, grain size, lattice imperfection and corrosion properties of Zn–Ni coatings deposited in alkaline bath.

* Corresponding author: ramanr@ktl.mii.lt

EXPERIMENTAL

Zn–Ni (12%) coatings 10 μm thick were electrodeposited on low carbon steel (C 0.05–0.12%, Mn 0.25–0.5%) samples, which had been polished mechanically to a bright mirror. An alkaline cyanide-free plating solution contained ZnO 10 g l^{-1}, NaOH 100 g l^{-1}, organic additives and a glycerine complex of Ni ions. The coatings were deposited at 25 °C and current density 3.5 A dm^{-2}. A detailed description of the plating bath and operating conditions have been presented elsewhere [5, 9–11].

Surface morphology studies were carried out with an AFM by an Explorer (VEECO-Thermomicroscopes) scanning probe microscope at atmospheric pressure and room temperature in a contact mode. A Si_3N_4 cantilever with the force constant of 0.032 N m^{-1} was used and the resolution of the images obtained was 300 × 300 pixels.

X-ray diffraction measurements were performed with a D8 diffractometer equipped with a Göbel mirror (primary beam monochromator) for Cu radiation. A step-scan mode was used in the 2-theta range from 30° to 75° with a step length of 0.02° and a counting time of 5 s per step.

The corrosion behaviour of coatings was investigated in 0.1 M NaCl + 0.1 M $NaHCO_3$ solution (pH 6.8) using a standard three-electrode system with a Pt counter electrode, a saturated calomel reference electrode and a PI-50 potentiostat.

RESULTS AND DISCUSSION

Chemical composition

Data on the composition, structure and corrosion behaviour of Zn–Ni coatings deposited in an alkaline bath by the direct current were presented in our previous studies [9, 11]. It was established there that the mentioned coatings consisted of the γ-$Zn_{21}Ni_5$ phase with the content of Ni close to ~12%, while their corrosion resistance under the conditions when the passivating corrosion product, film, forms (atmospheric corrosion or aqueous corrosion in a Cl^- ions containing buffered solution) appeared to be significantly higher than of pure Zn coatings [9].

The principal requirements for the pulse plated Zn–Ni alloy were absence of pitting damages and/or dendrites on the surface of the coating and the stability of its composition. The latter condition implies a variation of Ni content in the alloy between 10 and 15%. A lower amount of Ni in the alloy is accompanied by a dual phase formation, while a higher one causes the loss of the sacrificial protection effect of the coating.

The influence of pulse and reverse plating parameters (cathodic peak current density (i_p), current on-time (t_{on}), current off time (t_{oof}) and anodic peak current density (i_a)) on the amount of Ni in the alloy are presented in Fig. 1. Electrodeposition conditions affected significantly the composition of Zn–Ni alloy. The increase in i_p and t_{off} caused an increase, while the increase in t_{on} and i_a, in contrary, led to a decrease in Ni content in the alloy. The values of i_p lower than 1 A cm^{-2} were not acceptable, because they caused reduction of Ni content below 10%, while application of t_{on} lower than 0.1 ms and i_a lower than 0.1 A cm^{-2} resulted in alloy formation with a Ni content overcoming 15%. The latter case was not acceptable in this study, either. The presented dependences (Fig. 1) validate the optimal range of pulse plating parameters, which assured the desirable composition of Zn–Ni alloy.

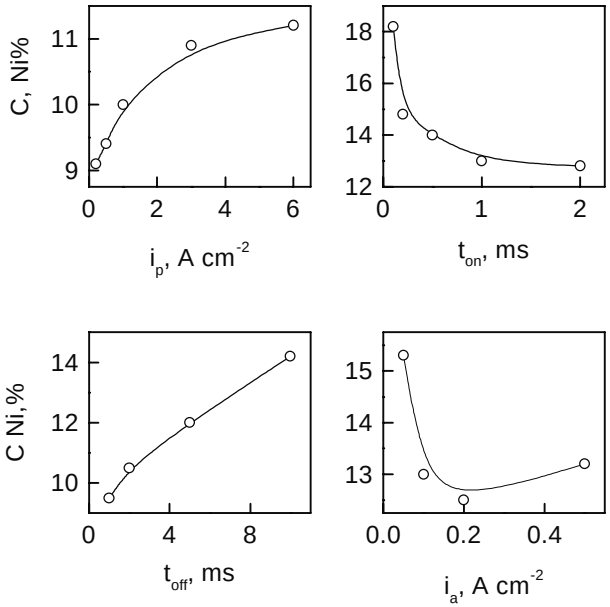

Fig. 1. Effect of pulse plating parameters on Zn–Ni alloy composition

Phase composition

The influence of pulse plating parameters on the phase composition of the deposited alloy can be determined from XRD data. Figure 2 shows XRD patterns of Zn–Ni coatings deposited under various

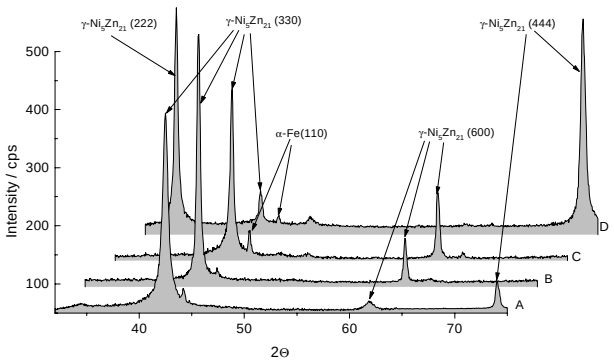

Fig. 2. XRD patterns of Zn–Ni coatings obtained by pulse plating under various cathodic current peak (i_p) densities (A cm^{-2}): *A* – 0.2, *B* – 1, *C* – 3, *D* – 6

i_p conditions. The variation of other pulse and reverse plating parameters (t_{on}, t_{off} and i_a) did not cause the appearance of any new characteristic features in the obtained diffractograms, therefore, they are not presented here.

All the Zn–Ni samples showed sharp peaks corresponding to the base metal (Fe) and to γ-$Zn_{21}Ni_5$ phase. No other Zn–Ni alloy phases were detected to be present in the electrodeposited coatings. This fact implies that under applied pulse and reverse plating conditions the deposited alloy consisted of a single γ-$Zn_{21}Ni_5$ phase.

An additional diffraction line characteristic: a full width at half-maximum (FWHM) W_{FWHM} was measured and the obtained data will be presented and discussed below.

Surface morphology

Surface morphology studies of Zn–Ni coatings were based on AFM measurements. Investigations on the μm level (20 × 20 μm scanned surface area) have shown that d.c. plated coatings (deposited at 3.5 A dm^{-2} current density) consisted of agglomerations of nodular crystallites (Fig. 3a). The dimension of such agglomerations varied between 1.1 and 3.2 μm, (average 2.0 μm), meanwhile the dimensions of the individual crystallites (Δ_{Cr}) ranged between 0.5 and 1.8 μm (the average value 0.92 μm).

The ultrafine-grained structure was determined from the 500 × 500 nm scanned surface area (Fig. 4a) and the grain size (Δ_{gr}) of d.c. deposited coatings varied between 70 and 180 nm, with the average 90 nm value.

The influence of pulse plating parameters on the morphology of electrodeposited Zn–Ni coatings can be observed from the images presented in Figs. 3 and 4 b–d. The average crystallite dimensions, grain size, as well as the root-mean-square roughness (R_{rms}) values were determined from the AFM measurements and the obtained data are presented in Fig. 5 and Table.

The morphology of Zn–Ni alloys deposited by pulse and reverse plating appeared to depend rigorously on the plating parameters. The characteristic feature of these coatings was the lack of crystallite agglome-

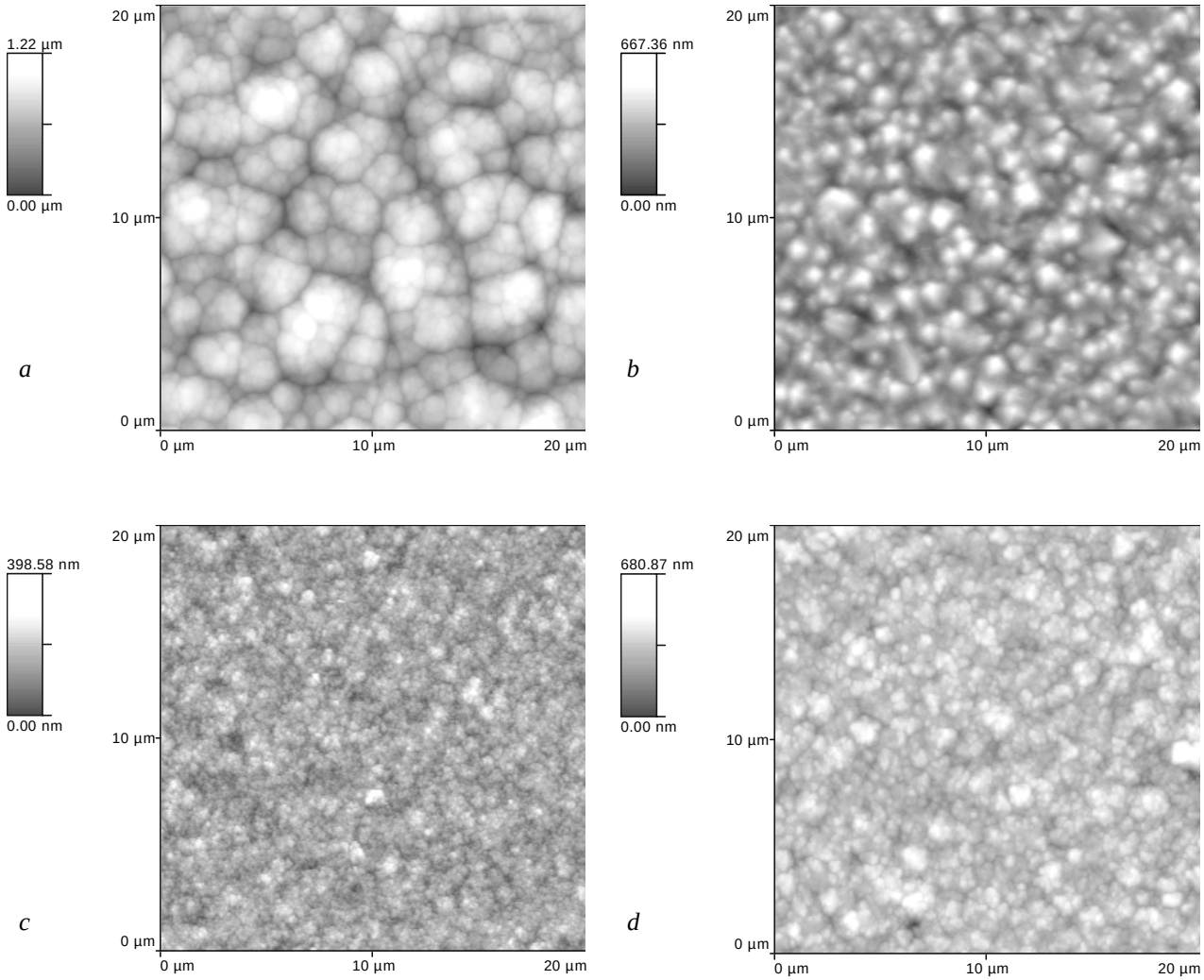

Fig. 3. Surface morphology of Zn–Ni coatings deposited under various i_p values (A cm^{-2}): *a* – d. c. plated coating, *b* – 0.5, *c* – 3, *d* – 6. The scanned area 400 $μm^2$

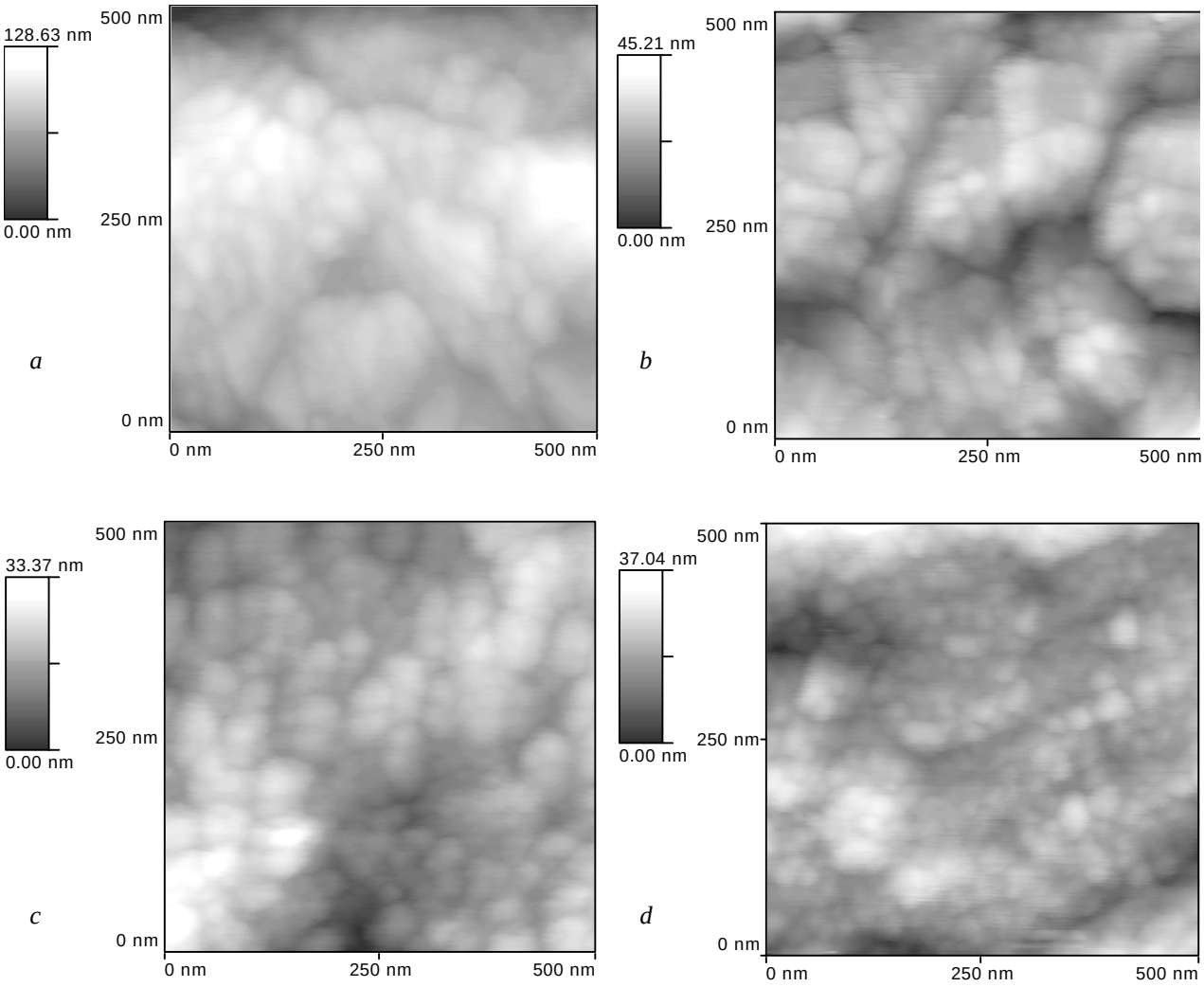

Fig. 4. Surface morphology of Zn–Ni coatings deposited under various i_p values (A cm^{-2}): *a* – d. c. plated coating, *b* – 0.5, *c* – 3, *d* – 6. The scanned area 0.25 μm^2

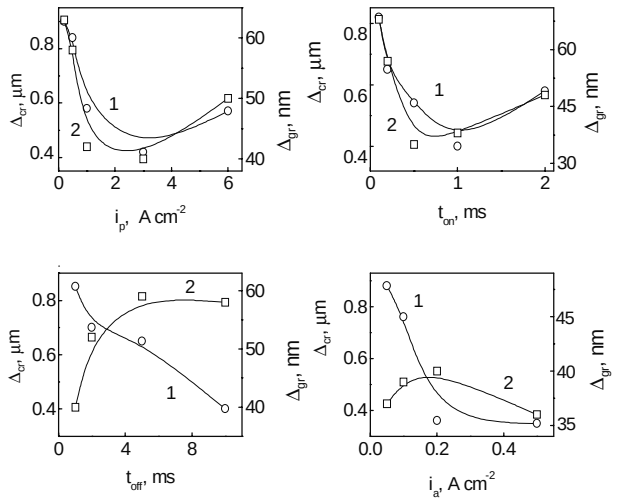

Fig. 5. Effect of pulse plating parameters on the crystallite radius (Δ_{cr}, μm) (1) and grain size (Δ_{gr}, nm) (2) of pulse plated Zn–Ni coatings

rations, which were observed for d.c. plated samples. The surface of pulse plated Zn–Ni coatings appeared to consist of globular crystallites. The variation of plating conditions (the increase in i_p, t_{on}, t_{off} and i_a) caused a significant reduction in their dimensions, and as a result the surface morphology underwent modification from a globular to a fine-grained film.

The increase in the overpotential enhances the free energy to form new nuclei, which result in a higher nucleation rate and a smaller grain size. Therefore, an increase in i_p in the pulse plating of metals usually causes a decrease in the grain size. A similar effect was also observed for Zn–Ni pulse electrodeposits. An increase in i_p values from 1 to 3 A cm^{-2} caused a slight reduction in the average Δ_{cr} values from 0.58 μm up to 0.42 μm and reduction on the average Δ_{gr} from 42 nm up to 40 nm (Fig. 5). The further increase in i_p (>3 A cm^{-2}) caused dendrite formation on the coatings surface, which was accompanied by an increase in the corresponding Δ_{cr} and Δ_{gr} values. The lowest R_{rms} values of the mentioned samples varied between 60 and 40 nm and were obtained when i_p exceeded 3 A cm^{-2} (Table).

The variation in the t_{on} parameter enabled to obtain Zn–Ni alloys with a lower surface roughness.

Table. **Surface roughness of pulse and reverse plated Zn–Ni coatings**

Electrodeposition parameter		R_{rms}, nm
i_p, A cm^{-2}	0.2	144
	0.5	82
	1	52
	3	40
	6	61
t_{off}, ms	1	48
	2	58
	5	45
	10	30
t_{on}, ms	0.1	84
	0.2	21
	0.5	23
	1	20
	2	37
i_a, A cm^{-2}	0.05	13
	0.1	11.5
	0.2	13.5
	0.5	15

The average R_{rms} values around ~20 nm were obtained when t_{on} varied between 0.2 and 1 ms. The application of the t_{on} parameter higher than 0.2 ms produced Zn–Ni surfaces with spherical crystallites and relatively undefined grain boundaries. Meanwhile, the influence of t_{on} on Δ_{cr} and Δ_{gr} appeared to be similar to that of the previous (i_p) case, as a decrease in Δ_{cr} to 0.40 μm and Δ_{gr} to 35 nm was obtained at 1 and 0.5 ms t_{on} values, respectively. The onset of dendrite formation on the alloy surface was observed when t_{on} higher than 1 ms was applied. A corresponding increase in Δ_{cr} and Δ_{gr} values was also observed under the same conditions.

In pulse plating there is no applied current during the t_{off} period. Local corrosion cells can be formed during this period if it is long enough, as has been stated in several studies [14]. The t_{off} variations influenced formation of Zn–Ni alloy coatings with the lowest values of around Δ_{cr} and Δ_{gr} 0.4 μm and 40 nm, respectively. Surface flaws typical of local corrosion attack were observed on the surface when t_{off} exceeded 5 ms. This fact limited the use of higher t_{off} values.

Application of the reverse current peak produced significantly smoother coatings with R_{rms} close to 11–15 nm. The use of i_a in the deposition program caused formation of spherical crystallites with relatively undefined grain boundaries. The smallest crystallites (Δ_{cr} ~ 0.4 μm) were obtained at $i_a \geq 0.2$ A cm^{-2}, while the lowest values of Δ_{gr} (~35 nm) were observed for coatings deposited under i_a 0.05 A cm^{-2}. However, the further increase in i_a (>0.2 A cm^{-2}) caused formation of structural defects originated most probably by the alloy ionization process.

It may be stated, therefore, that application of pulse and reverse current in electrodeposition of Zn–Ni alloy in alkaline solution results in a significantly smoother surface with relatively indefinite grain boundaries and a reduction in the grain size from ~130 nm for d.c. plated up to 30–40 nm for pulse plated samples.

Corrosion behaviour and structure relationship

Corrosion behaviour of pulse plated Zn–Ni coatings was investigated in a naturally aerated NaCl + $NaHCO_3$ solution with pH 6.8 by means of anodic polarization measurements. It is known, however, that the corrosion rates measured electrochemically are in error with atmospheric data, mainly because of the presence of corrosion products on the surface. Zn alloy corrosion in unbuffered Cl^- solution occurs with the formation of oxide film having a porous structure [15]. However, in HCO_3^- containing media the oxide film is supposed to be more compact, adherent and less soluble, thus exhibiting a passivating character [16]. Aqueous corrosion data for Zn alloys in HCO_3^- containing media correlate well with atmospheric corrosion data [9]. The corrosion currents were determined from Tafel plot extrapolation and the data obtained are presented in Fig. 6. The same figure contains data on W_{FWHM} of the diffraction line (110) of Zn–Ni alloys electrodeposited under various conditions.

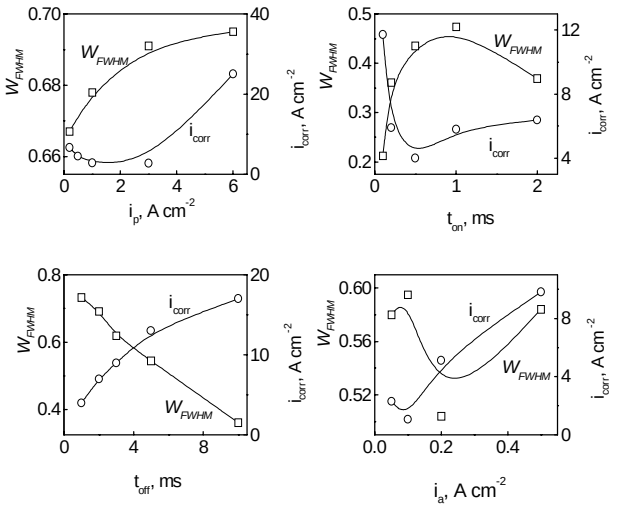

Fig. 6. Effect of pulse plating parameters on the corrosion current of Zn–Ni alloy coatings in NaCl + $NaHCO_3$ solution and the values of a full width at half-maximum (FWHM) W_{FWHM} of the diffraction line (110)

The relationship of surface morphology and corrosion behaviour (i_{corr}) of Zn–Ni coatings are not unambiguous. Generally, the lower values of Δ_{cr} and Δ_{gr} yields lower i_{corr} values, as it can be observed from i_p and t_{on} variations. However, several exceptions can be observed as well. In the case of t_{off}

and to some extent of i_a variations the increase in these parameters was accompanied by the reduction in Δ_{cr} and increase in Δ_{gr}. Under the same conditions the increase in coatings i_{corr} was detected. This fact implies the dominant influence of the grain size on the corrosion behaviour of alloy. The lowest values of Δ_{gr} for electrodeposited Zn–Ni alloy under all applied plating conditions varied around 35–40 nm, while the corresponding i_{corr} values ranged between from 1.5 to 4.0 10^{-6} A cm^{-2}, being the minimal ones for samples deposited with a pulse and reverse current. It seems that not only the grain size of the alloy is responsible for the corrosion properties of the coating.

The corrosion process is essentially a surface phenomenon, thus, it might be strongly related to crystalline perfection, *e.g.*, highly stepped metal surfaces, since the presence of dislocations makes the steps indestructible. It is reasonable hence, to argue that the lattice distortions must be important in the corrosion process.

As is evident from the data presented in Fig. 6 the higher values of W_{FWHM} usually are related to lower i_{corr} values of Zn–Ni alloy and *vice versa*. This statement is clearly evident for i_p, t_{on} and t_{off} variations, however, only up to a certain number of these parameters. The manifesting discrepancies are most probably related with formation of structural defects, *e.g.*, under i_p higher than 3 A cm^{-2} the outset of dendryte development might be responsible for higher corrosion rates of the coating, in spite of the highest W_{FWHM} values shown by this alloy. The increasing values of W_{FWHM} during the reverse current pulse application, when i_a exceeded 0.2 A cm^{-2}, were accompanied also by the highest values of i_{corr}, most probably due to corrosion damages on the surface.

X-ray diffraction line broadening is recognized to be caused by crystallite size and lattice strains [17]. In general, the grain size of Zn–Ni electrodeposits lies in the range for which X-ray diffraction is quite insensitive to its variations, so the observed line broadening will be affected mostly by lattice imperfections. Coatings with high values of W_{FWHM} show low corrosion rates. It implies that coatings with a higher number of lattice imperfections possess higher corrosion resistance. A similar assumption was done in our previous work with the following explanation. A decrease in crystalline perfection affects the surface reactivity and usually increases it. A higher surface activity of certain Zn–Ni alloys, and hence the metal structure, might be the precursor for oxide film formation with a high content of Zn hydroxide and poor crystallinity. The amorphous structure and lower electron conductivity of hydrated Zn oxide compared to those of Zn oxide made such alloys more stable in corrosion environments where passive films formed on the metal surface.

CONCLUSIONS

The composition of pulse plated Zn–Ni alloy coatings depended on the plating parameters: an increase in cathodic current peak density (i_p) and time off period (t_{off}) caused an increase, while an increase in anodic (reverse) current peak density (i_a) and time on period (t_{on}) a decrease in Ni content in the alloy. All pulse plated Zn–Ni coatings, in spite of the differences in their composition, consisted of a single γ Zn–Ni phase.

Pulse and reverse plating of Zn–Ni alloy in alkaline solutions results in formation of a significantly smoother surface with relatively indefinite grain boundaries and reduction in the grain size from ~90 nm for d.c. plated up to 35–40 nm for pulse plated samples.

Zn–Ni alloys with lower grain size values and without macrostructural defects (outset of dendryte, areas of corrosion attack) exhibited a higher corrosion resistance. Lattice imperfection, grain size and grain uniformity are the main factors that determine the corrosion behaviour of Zn–Ni coatings.

Received 16 November 2004
Accepted 26 November 2004

References

1. K. R. Baldwin, M. J. Robinson and C. J. E. Smith, *Corros. Sci*., **35**, 1267 (1993).
2. L. Fedrizzi, R. Fratesi, G. Lunazzi and G. Roventi, *Surf. Coat. Technol*., **53**, 171 (1992).
3. G. D. Wilcax and D. R. Gabe, *Corros. Sci*., **35**, 1251 (1993).
4. W. Kautek, M. Sahre and W. Paatsch, *Electrochim. Acta*, **39**, 1151 (1994).
5. M. A. Pech-Canul, R. Ramanauskas and L. Maldonado, *ibid*., **42**, 255 (1997).
6. J. B. Bajat, M. D. Maksimovic, V. B. Miskovic-Stankovic and S. Zec, *J. Appl. Electrochem*., **31**, 355 (2001).
7. Ch. Hu, Ch. Tsay and A. Bai, *Electrochim. Acta*, **48**, 907 (2003).
8. A. M. Alfantazi, J. Page and U. Erb, *J. Appl. Electrochem*., **26**, 1225 (1996).
9. R. Ramanauskas, *Appl. Surf. Sci*., **153**, 53 (1999).
10. R. Ramanauskas, L. Gudaviciute, L. Diaz-Ballote, P. Bartolo-Perez and P. Quintana, *Surf. Coat. Technol*, **140**, 109 (2001).
11. R. Ramanauskas, R. Juskenas, A. Kalinicenko and L. F. Garfias-Mesias, *J. Solid State Electrochem*., **8**, 416 (2004).
12. Y. Tsuru and M. Tanaka, *Denko Kagaku*, **64**, 112 (1996).
13. K. Kondo, M. Yokoyama and K. Shinohara, *J. Electrochem. Soc*., **142**, 2256 (1995).
14. N. V. Mandich, *Metal Finishing*, **98**, 375 (2000).
15. T. E. Graedel *J. Electrochem. Soc*., **136**, 193C (1989).
16. R. Guo, F. Weinberg and D. Tromans, *Corrosion*, **51**, 356 (1995).
17. D. J. Balzar, *J. Appl. Cryst*., **25**, 559 (1992).
18. J. Giridhar and W. J. Ooij, *Surf. Coat. Technol*., **52**, 17 (1992).

Rimantas Ramanauskas, Laima Gudavièiûtë, Aleksandras Kalinièenko, Remigijus Juðkënas

IMPULSINËS IR REVERSINËS ELEKTROS SROVËS ÁTAKA ZN IR ZN LYDINIØ STRUKTÛRAI IR KOROZINËMS SAVYBËMS.

1. ZN–NI

S a n t r a u k a

Tirta impulsinës elektros srovës parametrø átaka pavirðiaus morfologijai, kristalitø dydþiui, gardelës defektingumui ir Zn–Ni lydiniø korozinëms savybëms. Lydiniø dangos nusodintos ið ðarminio necianidinio elektrolito, turinèio glicerininá Ni jonø kompleksà. Pavirðiaus morfologiniams tyrimams taikyta atomo jëgos mikroskopija, faziø sudëties bei tekstûros analizei panaudoti rentgeno difrakciniai matavimai. Nustatyta, kad Zn–Ni dangos, gautos impulsine elektros srove, sudarytos ið γ-$Zn_{21}Ni_5$ fazës, kurios sudëtis priklauso nuo dengimo parametrø. Lydinio gardelës defektingumas ir kristalitø dydis yra pagrindiniai veiksniai, sàlygojantys dangos korozines savybes.